Coupled global-local modelling for dynamic submarine power cables

Rachel Nicholls-Lee, Philipp R. Thies, Lars Johanning

Abstract— **Conventional power transmission cables have been designed to operate in conditions that differ considerably from those experienced by cables servicing floating offshore renewable energy (ORE) device. Cables attached to floating platforms are subject to greater levels of mechanical and electrical stress due to the motion of the platform in a highly energetic offshore environment and are termed dynamic cables. The combination of the different loads from waves, wind and currents, in shallower waters are complex and need to be assessed through a combination of coupled numerical models and experimental tests.**

Global analyses, assessing the overall motions of the floating platform, moorings and cables, are carried out to provide data to inform the cable design process. Such analyses are highly dependent on the input of local structural response coefficients which are available only through detailed local structural analysis numerically and/or experimentally. There is a strong need to gain a better understanding of the local structural assessment of cable cross-sections and the coupling of the data attained through the local assessments with the global modal.

This work incorporates a coupled global-local numerical model of a dynamic subsea cable attached to a floating point-absorber buoy. The results indicate the sensitivity of the global analysis to the locally determined structural results, primarily bending stiffness and tensile stiffness. In the case of the South West Moorings Test Facility (SWMTF) buoy and the lightweight composite armoured cable, bending stiffness is a key governing parameter and axial stiffness is not a governing parameter. The paper will be of use to researchers and practitioners in the areas of cable designers, technology development and design certification.

Keywords—**dynamic subsea power cable, coupled modelling, bend stiffness, axial stiffness, governing design parameters.**

I. Introduction

The design, installation and operation of high power static subsea cables are well understood mature technology areas [1]. One of the missing elements in the power transmission system, is the portion of cable that links the floating production facility with the static cable on the seabed, the substation, or a floating substation to shore. Cables must now have the ability to support increased mechanical loads caused by deeper waters, effectively supporting the cable weight, and the movement of the floating vessel or platform. They must also be able to tolerate fatigue associated with cyclic load changes that occur during their induced movement in the water column.

Floating ORE platforms show some similarities with semi-submersible oil platforms, but have very different motions, as their geometry and wave and tidal loads are significantly different. Extensive research has been done in terms of evaluating the lifetime for flexible risers and umbilicals in relation to fatigue for the oil and gas industry [2]. Considerably less work has been reported regarding the lifetime of dynamic flexible cables for floating Marine Renewable Energy (MRE) platforms. The combination of the different loads from waves, wind, currents, and more are complex and need to be assessed through a combination of coupled numerical models and experimental tests – key to this is the verification of fatigue strength of the cable [3].

A dynamic power cable is susceptible to fatigue or over bend when there is an abrupt change in bending stiffness [3], for example where bend stiffeners, buoyancy floats and touchdown protection are present, Fig. 1.

PAPER ID. This work was funded through the EPSRC Supergen Offshore Renewable Energy (ORE) hub [EP/S000747/1].

R. Nicholls-Lee is a Research Fellow in the Renewable Energy Group, University of Exeter, College of Engineering, Mathematics and Physical Sciences, SERSF Building, Penryn Campus, Treliever Road, Cornwall, TR10 9FE, U.K. (R.F.Nicholls-Lee@exeter.ac.uk).

P.R. Thies is an Associate Professor of Offshore Reliability in the Renewable Energy Group, University of Exeter, College of Engineering, Mathematics and Physical Sciences, SERSF Building, Penryn Campus, Treliever Road, Cornwall, TR10 9FE, U.K. (P.R.Thies@exeter.ac.uk).

L. Johanning is a Professor of Ocean Technology in the Renewable Energy Group, University of Exeter, College of Engineering, Mathematics and Physical Sciences, SERSF Building, Penryn Campus, Treliever Road, Cornwall, TR10 9FE, U.K. (L.Johanning@exeter.ac.uk).

ISSN 2309-1983

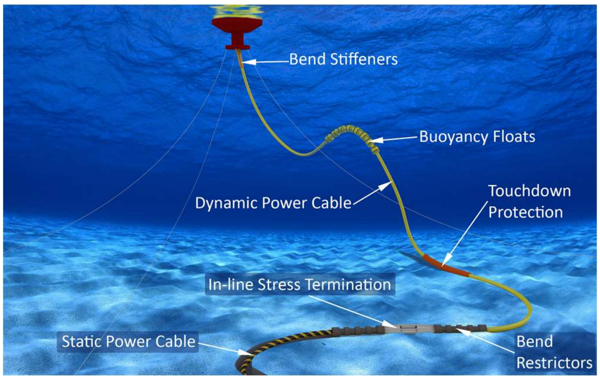

Fig. 1. Key elements of a dynamic subsea power cable assembly.

There are mainly three causes of mechanical failure in marine power cables applied to marine energy applications: maximum axial tension, over bending, and fatigue under extreme cyclic loads [4]. Previous work has shown that the local effects in the cable cross-section play an important role in the assessment of fatigue life [3]. A good understanding of the internal structure of a subsea cable, and interaction between the layers, is integral to the development of robust and reliable, high voltage, dynamic, subsea cables.

Global analyses, assessing the overall motions of the floating platform, moorings and cables, are often carried out to provide data to inform the cable design process. Such analyses, however, are highly dependent on the input of local structural response coefficients which are available only through detailed local structural analysis numerically and/or experimentally. There is a strong need to gain a better understanding of the local structural assessment of cable cross-sections and the coupling of the data attained through the local assessments with the global modal.

Kuznecovs et al [5] developed a methodology for the dimensioning of complex cables with multiorder helix configurations. They assessed the strands of the conductor core of a dynamic subsea cable design suitable for a floating, point-absorber wave energy converter (WEC) and determined a prediction of fatigue life for early-stage design work. The focus was on a local level and use of S-N curves to predict fatigue. On a more global level Thies et al [6] assessed the sensitivity of various parameters and potential failure modes on a dynamic submarine power cable attached to a generic point absorber wave buoy in OrcaFlex [7]. These included environmental parameters (tidal range, tidal current direction, tidal current speed) and cable design parameters (cable weight, cable shape configuration).

This paper builds on the previous experience in fatigue assessment in subsea cables with a coupled global-local model of a 66kV dynamic subsea power cable attached to the SWMTF Buoy [8]. The work investigates the sensitivity of the global model to locally determined bend stiffness and axial stiffness. The paper is structured as follows. Section II describes the numerical model setup of the floating buoy and the cable, outlining both the global and local model. Section III presents the results and discussion. The main conclusions are drawn in section IV.

II. NUMERICAL MODELS

This section describes the components and associated parameters and set up of the point absorber buoy, mooring system and dynamic cable.

A. SWMTF Buoy

The South West Moorings Test Facility (SWMTF) buoy (Fig. 2) was developed with the intention of providing real sea condition testing and performance analysis, uncertainty reduction, and to facilitate the design of future WEC mooring systems and components.


Fig. 2. SWMTF buoy installed at sea.

Several studies have investigated various mooring systems and components both numerically and experimentally at various scales [8, 9]. The buoy and mooring spread have the principal particulars shown in Table 1.

TABLE I
PRINCIPAL PARTICULARS OF THE SWMFT BUOY

Particular	Value	Unit
BUOY		
Diameter	2.9	m
Depth (to base)	1.42	m
Depth (to keel)	2.45	m
Centre of Gravity (from keel)	1.13	m
Draught	1.66	m
Displacement	3250	kg
MOORINGS		
Anchor (drag embedment)	1100	kg
Ground Chain (32 mm stud link)	5	m
Riser Chain (24 mm stud link)	36	m
Rope Tail (44 mm Jacketed parallel lay nylon)	20	m

B. Dynamic Power Cable

The power cable assessed in this work is a notional 72.5kV dynamic power cable with aluminium conductors, XPLE insulation and a novel, lightweight composite armour, Fig. 3 [10].

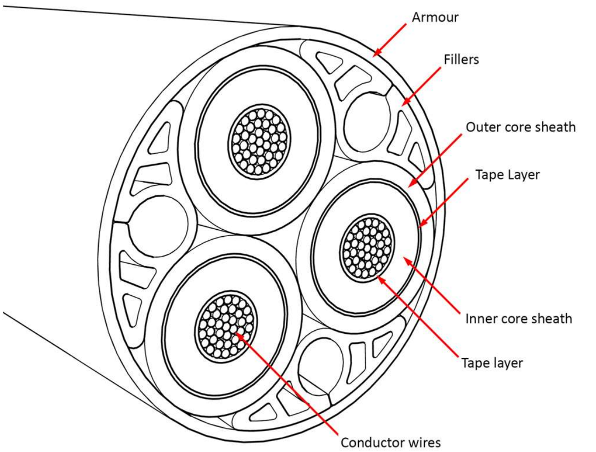

Fig. 3. Dynamic cable schematic [10].

The use of aluminium for the conductors allows for a lower cost and weight, favouring dynamic application in the offshore renewable sector. The power cable has an outer diameter of 122mm and a wet weight of 5.5kg/m.

The bending stiffness and axial stiffness have been determined through a local structural model for input into the global model.

C. Global Numerical Model

The global scenario was modelled in OrcaFlex [9]. The model consists of the SWMFT Buoy, associated mooring spread, dynamic cable and cable floats, Fig. 4.

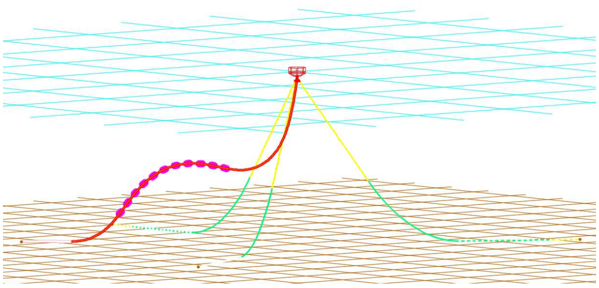

Fig. 4. Global OrcaFlex model screenshot

The cable floats have been modelled discretely, as opposed to smearing the properties over the central length of cable. Each float has an outer diameter of 0.5m, length of 0.5m and density of 291kg/m^3. The buoyancy has been distributed along the central section of cable in a configuration previously determined to minimise tension and maximise bending radius [6].

One of the more severe sea states for the SWMTF Buoy has been used for the assessment of the effect of locally derived bending stiffness and axial stiffness values of the dynamic subsea power cable, the details of which are shown in Table 2. These values correspond to the highest observed from long-term sea trials of marine energy devices at the SWMFT buoy site [11-13]. In this study, a 3 hour irregular wave train was generated based on a JONSWAP Spectrum using the data in Table 2. Then a shorter section of 200 seconds was selected that contained the maximum wave height of the wave train. This section of the wave train was then used for simulation where axial and/or bending stiffness was changed for consistency.

TABLE 2
ENVIRONMENTAL PARAMETERS

Parameter	Value	Unit
Water Depth	30	m
Significant wave height (Hs)	3.5	m
Wave Period (Tp)	8	s
Wave Spectrum	JONSWAP	

Fig. 5 shows the effective tension along the cable when assessed under the environmental conditions detailed in Table 2. Point A denotes the attachment point to the SWMTF buoy, points B the end of the initial bend restrictor, point C the start and point D the end of the central section of the cable with the discrete buoyancy floats, and point E shows where the cable touches down on the seabed. The effective tension represents a composite tension, which incorporates the effects of external fluid pressure, eqn. (1).

$$T_{eff} = T_{wall} + p_e a_e \tag{1}$$

Where T_{eff} is effective tension in kN, T_{wall} is the wall tension in kN, p denotes pressure terms in kPa, a is the cross-section area in m^2 and the subscript e denotes external.

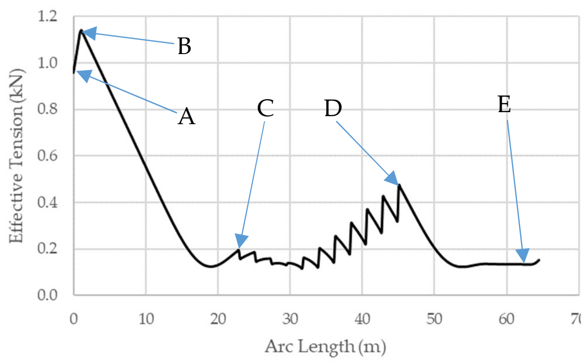

Fig. 5. Effective tension along the length of the cable, the saw-tooth effect between C and D is due to the floats being modelled discretely.

D. Local Numerical Model

The local model of the cable was developed in ANSYS Mechanical (2020 R2). Subsea power cables are highly complex structures and modelling the cable in full detail results in many millions of computationally intensive contact elements. In order to solve the simulations in a reasonable time frame the cable was simplified, as shown in Fig. 6, by merging the individual core wires and removing the tape layers. Even in this simplified state the model took over 10 hours to solve on a high performance computer with 128GB of RAM with 16 cores. Investigations as to the effects of merging these layers will be carried out in future work.

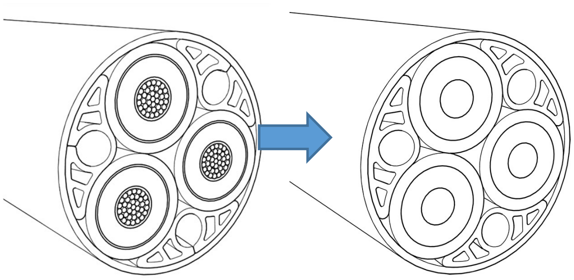

Fig. 6. Dynamic cable geometry simplification for analysis.

The cable was constrained as a cantilever beam, again to bring the simulation time to a reasonable level. Using simply supported constraints results in an increase in solution time of 4x, to 40 hours, again on the 128GB RAM supercomputer. A mesh sensitivity study was carried out to determine the parameters at which the simulation results converged, whilst using the minimum necessary amount of computational memory to achieve this. Five different meshes were analysed, with Fig. 7 showing the cross section of the coarsest and finest meshes.

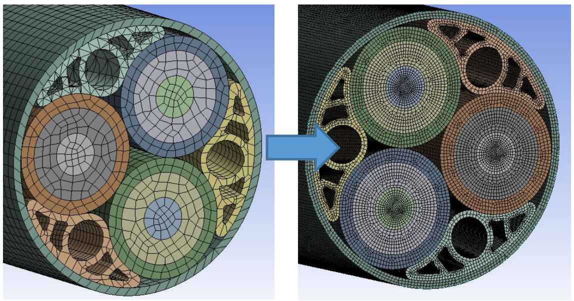

Fig. 7. Mesh sensitivity study – coarse to fine

The convergence of both maximum stress and maximum deflection is show in Fig. 8.

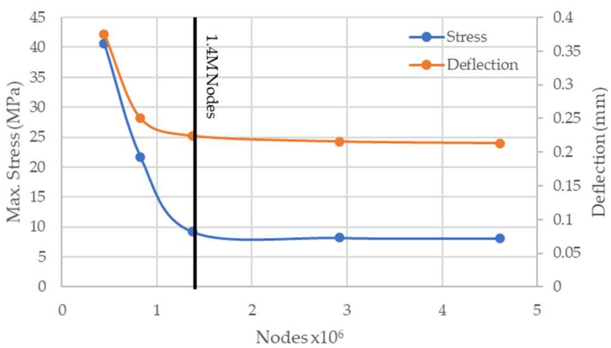

Fig. 8. Mesh convergence of maximum stress and deflection

A mesh was then chosen with 1.4 million nodes which resulted in converged results, but also minimised solution time and ensured a minimum of two elements in the through thickness of all components, Fig. 9.

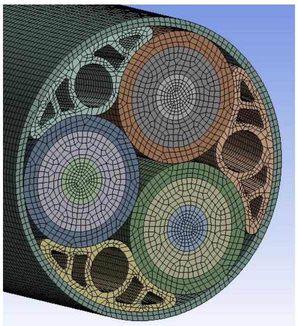

Fig. 9. Mesh convergence of maximum stress and deflection

The cable was treated as a cantilever beam to determine the bending stiffness, fixed on the armouring only at one end and with a force applied at the other. At this stage in the design process this was deemed sufficient, as more realistic (simply supported or four-point bending) constraints are highly computationally intensive and will be investigated in future work.

To determine the axial stiffness, all layers of the cable were fixed at one end with a tensile force applied at the other.

III. Results and Discussion

This section discusses the effect of discrete buoyancy float modelling, and the effect of changing both bending stiffness and axial stiffness of the cable, as determined in the local analyses, on the global model.

E. Discrete vs Distributed Buoyancy

The buoyancy floats have been modelled in OrcaFlex as both discrete floats and a section of cable with distributed properties, Fig. 10. The distributed cable section applies buoyancy using a line section that has the equivalent smeared properties of the line and buoyancy modules combined. This approach is less computationally intensive and appropriate for the early design stage. Buoyancy is applied as discrete modules attached to the line for the individual floats. This is more computationally expensive; however, in latter stages of design enables assessment that the module size and pitch do not allow excessive sag of the cable between the modules.

The 'base' case for the cable was used in these analyses with manufacturer stated values of bending stiffness and axial stiffness of 6.24kNm^2 and 42.1MN respectively.

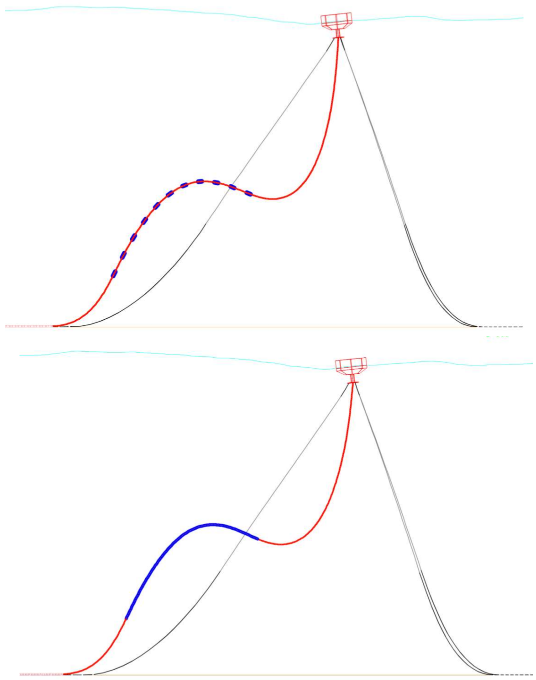

Fig. 10. Discrete floats (top) and distributed buoyancy (bottom)

Fig. 11 shows a plot of the maximum, mean and minimum effective tension in the cable against arc length comparing both the discrete and distributed approaches. The early indications of 'curtain-railing' can be seen in the central section where the individual floats have been applied. The distributed method tends to underestimate the maximum tension and overestimate the minimum tension when compared to the discrete method. The divergence increases with the length of the buoyancy section. The mean tension shows good agreement. The maximum load is critical for assessment of the ultimate tensile strength of the cable, and the minimum load for design against compressive forces. The distributed method is not conservative, i.e. not suitable for critical designs regarding compression and ultimate tensile strength, and therefore not suitable beyond the early design stage.

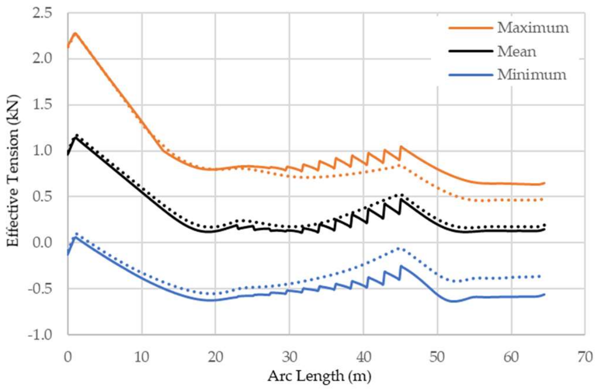

Fig. 11. Minimum, mean and maximum effective tension along the cable showing a comparison of discrete (solid lines) and distributed (dotted lines) buoyancy.

The distributed method has been used for the remainder of this work, as it is an early-stage design assessment of the governing design parameters, with values for the mean effective tension in each case utilised for comparison.

Typically, early-stage global modelling of dynamic subsea power cables utilises a single, fixed, value for many of the cable governing design parameters such as axial stiffness and bending stiffness. While cable hysteresis is recognised as a physical characteristic, determining accurate hysteresis curves for each cable is computationally and experimentally demanding. Hence a single representative value is commonly used to investigate early global design parameters such as environmental and metocean effects on the overall system. The following results and discussion consider the magnitude of the effect of variation of values of axial and bending stiffness on the cable response.

F. Axial Stiffness

Various values of axial stiffness were determined through the local model by applying a range of loads to a 1 metre length of cable. Figs. 12 and 13 show typical plots of the deflection and stress on the cable section when under tension. These plots are shown without values for confidentiality. The internal helical layup is apparent in both cases.

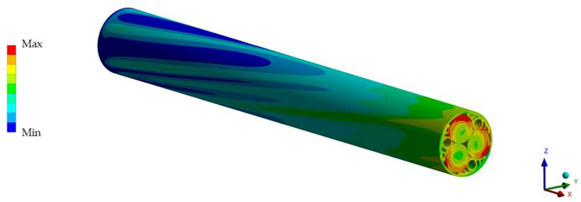

Fig. 12. Typical deflection plot of the cable modelled under tension.

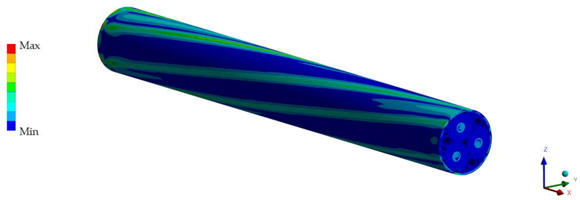

Fig. 13. Typical Von Mises stress plot of the cable modelled under tension.

The axial stiffness determined through the local model was lower than the base case axial stiffness for all applied loads. At an applied load of 5 kN the axial stiffness was 25.9 MN, almost half the base case 42.1 MN.

Fig. 14 shows the percentage change in both effective tension and curvature in the cable, for a range of values of axial stiffness, with the bending stiffness held constant at the base value of 6.24 kNm^2.

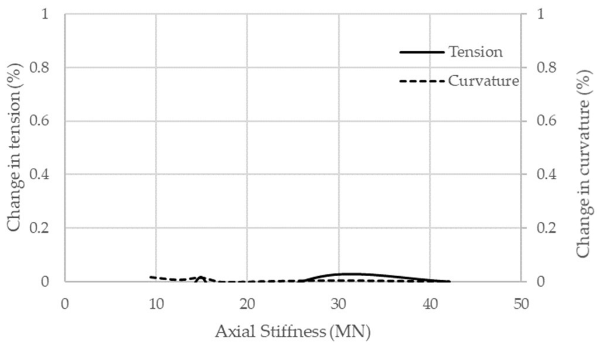

Fig. 14. Percentage change in effective tension and curvature in the cable with alteration of axial stiffness with bending stiffness constant at 6.24 kNm².

The effective tension and curvature results for each locally determined stiffness were the most extreme values determined throughout each simulation. Curvature is measured in rad/m, which was translated into a bending radius for results comparison. A maximum value of curvature equates to a minimum bending radius.

The change in curvature does not exceed 0.02%, and the change in tension does not exceed 0.03%. This is for a range of axial stiffness values. These are very small values. Repeating the global analysis for higher values of bending stiffness had little effect on these trends. Fig. 15 shows the percentage change in both effective tension and curvature in the cable, from the global model, for a range of values of axial stiffness, with the bending stiffness held constant at the base value of 25.88 kNm² – over 4x the base value. The same axis system scale has been used in both Figs. 14 and 15 for comparison.

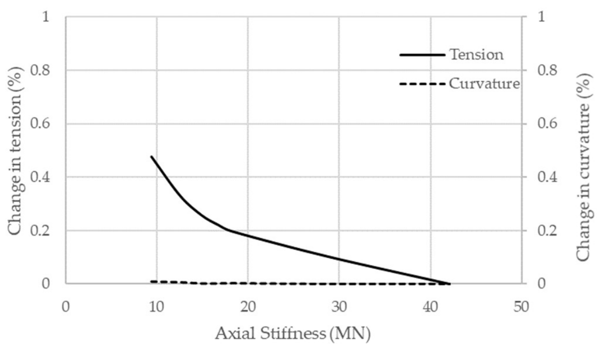

Fig. 15. Percentage change in effective tension and curvature in the cable with alteration of axial stiffness with the bending stiffness constant at 25.88 kNm².

In this case the change in curvature does not exceed 0.01%, and the change in curvature does not exceed 0.48%.

G. *Bending Stiffness*

Various values of axial stiffness were determined through the local model by altering the contact definition between the internal layers of a 1 metre length of cable. Figs. 16 and 17 show typical plots of the deflection and stress on the cable section when modelled as a cantilever beam. These plots are shown without values for confidentiality.

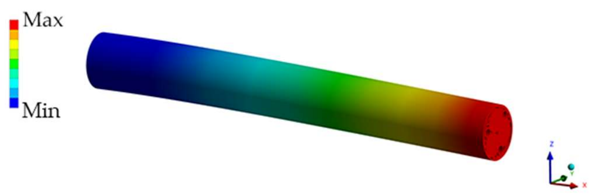

Fig. 16. Typical deflection plot of the cable modelled as a cantilever beam.

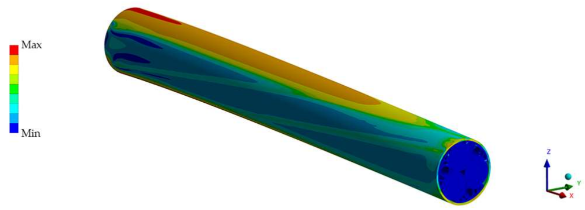

Fig. 17. Typical Von Mises stress plot of the cable modelled as a cantilever beam.

The bending stiffness determined through the local model was significantly larger than the base case bending stiffness for all applied loads. With an applied load of 1 kN the bending stiffness was 31.74kNm², over 5x the base case value of 6.24kNm² for a cable with a friction coefficient between the internal layers of 0.2 (chosen based on friction coefficients between polyethylene and other materials). Halving the length of the cable section analysed locally to 0.5m, increased this value to 39.10kNm², over 6x the base value. This indicates that the physical length of cable modelled in the local analyses is important and should be investigated further. The 0.5m long cable model took 15+ hours to solve on a PC with 64GB RAM, and 6 cores, and the 1m cable length 10 hours on a supercomputer with 128GB RAM and 16 cores – significant computational resource will be required to investigate sensitivity of the local model results to cable length.

Fig. 18 shows the change in both effective tension and curvature in the cable, from the global model, for a range of values of bending stiffness, with the axial stiffness held constant at the base value of 42.1 MN. Bending stiffness values from the local analysis were used, with some lower values nearer the base value of 6.24kNm² included to assess the effect on the global model results.

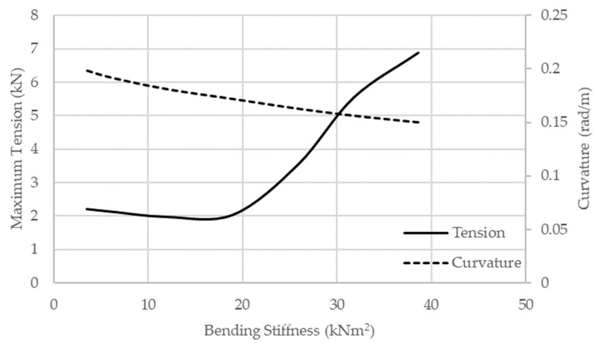

Fig. 18. Change in effective tension and curvature in the cable with alteration of bending stiffness with the axial stiffness constant at 42.1MN.

For lower values of bending stiffness (3.5-12 kNm^2) there is little change in tension, up to 6% variation. Increasing the bending stiffness to values determined through the local analysis has a significant change on the tension in the cable, with an increase up to 3x that of the base case stiffness value. It should be noted that the maximum tension in the cable was still relatively low at a value of 6.89kN, compared to the maximum allowable value of 120kN. Halving the axial stiffness, from the base case, and repeating the global analysis had very little effect on the tension and curvature of the cable. A maximum change of 0.86% was seen, which occurred at the lower values of bending stiffness.

The numerical estimation of bending stiffness has a range of uncertainties which are generally addressed through engineering factors and experimental calibration. To illustrate the extent of this, the element contacts can be modelled within an envelope of either "fully bonded" or "frictionless", which may change the bending stiffness by as nearly an order of magnitude. Thus the experimental testing is very important for calibration and verification of the local and global modelling.

The maximum curvature in the cable decreases slowly with an increase in bending stiffness, with a reduction of 21.6% for a bending stiffness of 38.59kNm^2 – over 6x the base bending stiffness value. The overall radius of curvature remained within acceptable values (in excess of 5m), with the stated minimum bend radius of the cable being 4.6m.

Literature reports variations between calculated, experimentally measured and manufacturer supplied values of both bending and axial stiffness [14, 15]. This shows a need for further investigation into determination of such properties for use at all design stages.

Previous initial work considering the effect of variation of bending stiffness and axial stiffness determined through local modelling and coupled with the global model indicated that cable curvature and tension are more sensitive to axial stiffness changes, especially at lower values of bending stiffness [16]. This work was carried out for a heavier dynamic subsea power cable, and a significantly larger floating wind platform, in deeper waters, with regular waves. This would indicate that the combination of cable mechanical properties with the floating platform and environmental parameters of the intended platform location is integral to understanding the key governing design parameters for each, individual situation and should be investigated further.

It is well understood that subsea power cables do not respond in a linear manner, both with respect to axial and bending stiffness [17, 18]. While it is common practise to hold these values fixed at the early design stage, particularly during global analyses, it has been shown that in various situations there can be a significant effect on the results of the global analysis with variation of stiffness values [16]. Investigation as to the sensitivity of the global analysis to non-linear definition of both bending and axial stiffness values determined through local analysis should be considered in the detailed design analysis.

IV. CONCLUSIONS

This paper has investigated the sensitivity of a global model of the SWMTF Buoy to locally determined bend stiffness and axial stiffness values for a 66kV dynamic subsea power cable.

The local model was found to be highly computationally expensive, and there is a necessity to ensure inputs and modelling methods are valid and accurate in order to utilise this approach effectively. The global model is fast for basic runs, and also useful for initial inputs for the local model.

At the early stage of the design process bending and axial stiffness values are commonly held fixed in the global model to assess the overall results. This work indicated that the global analysis of the SWMTF buoy was sensitive to changes in bending stiffness of the dynamic power cable, with up to a 3x increase in tension and a corresponding decrease of 21% in curvature in the cable for a 6x increase in bending stiffness. Altering axial stiffness had very little effect on both tension and curvature in the cable, less than 0.5% change. The conclusion is that, in the case of the SWMFT buoy and the lightweight composite armoured cable, bending stiffness is a key governing parameter and axial stiffness is not a governing parameter.

It was further found that the local model tended to predict significantly higher values of bending stiffness when compared the manufacturers stated value, and lower values of axial stiffness. It was also noted that the effect of altering bending and axial stiffness for a cable on a larger floating platform in deeper waters had a different effect on the tension and curvature in the attached cable. This indicates that detailed understanding of the cable properties in relation to the floating platform and environmental conditions is key to accurately assess the overall performance and to suitably predict the service life of floating offshore renewable energy components.

Further investigation into the effect of non-linear stiffness values in the global model, and cable length and contact behaviour in the local model will be carried out.

References

[1] T. Worzyk, "Submarine Power Cables: Design, Installation, Repair, Environmental Aspects", Springer-Verlag, Heidelberg, Berlin, Germany, 2009

[2] BS EN ISO 13628-5:2009 Petroleum and natural gas industries. "Design and operation of subsea production systems". Subsea umbilicals, https://doi.org/10.3403/30127454 (published 31/01/2010)

[3] K. Bakken, "Fatigue of dynamic power cables applied in offshore wind farms", *Department of Marine Technology*, Norwegian University of Science and Technology: Norway. pp. 135, 2019

[4] P.R. Thies, L. Johanning, and G.H. Smith, "Assessing mechanical loading regimes and fatigue life of marine power cables in marine energy applications". *Proceedings of the Institution of Mechanical Engineers, Part O: Journal of Risk and Reliability*, vol. 226, no. 1, pp. 18-32. 2012.

[5] A. Kuznecovs, et al., "A methodology for design and fatigue analysis of power cables for wave energy converters", *International Journal of Fatigue*, vol. 122, pp. 61-71, 2019.

[6] P.R. Thies, L. Johanning, C. Dobral, "Parametric sensitivity study of submarine power cable design for marine renewable energy applications", *Proceedings of the ASME 2017 36th International Conference on Ocean, Offshore and Arctic Engineering*, Trondheim, Norway, June 25-30, 2017.

[7] OrcaFlex v11.0f, "OrcaFlex Help", 2020 [Online] https://www.orcina.com/webhelp/OrcaFlex/Default.htm, Orcina Ltd. 2020 (accessed 7th January 2021)

[8] V. Harnois, et al, "Numerical model validation for mooring systems: Method and application for wave energy converters", *Renewable Energy*, vol. 75, pp. 869-887, 2015

[9] P.R. Thies, L. Johanning, V. Harnois, H.C.M. Smith, D. Parish, "Mooring line fatigue damage evaluation for floating marine energy converters: Field measurements and prediction", *Renewable Energy*, vol. 63, pp. 133-144, 2014

[10] G. Rinaldi, et al, "D.3.5 Results for local cable component analysis and fatigue modelling with input from global analysis", FLOTANT, H2020-LC-SC3-2018, 210115-FLT-WP3_D_3.5-v_0, January 2021

[11] V. Harnois, D. Parish, L. Johanning. "Physical measurement of a slow drag of a drag embedment anchor during sea trials", *Proceedings of the 4th international conference on Ocean Energy (ICOE)*, Dublin, Ireland; 2012.

[12] V. Harnois, L. Johanning, P.R. Thies, I. Bjerke, "On peak mooring loads and the influence of environmental conditions for marine energy converters", *Journal of Marine Science and Engineering*, vol. 4, iss. 2, p. 29, 2016

[13] L. Johanning, A.W. Spargo, D. Parish, "Large scale mooring test facility - a technical note", *Proceedings of the 2nd international conference on Ocean Energy (ICOE)*, Brest, France; 2008.

[14] K. Papailiou, "Bending of helically twisted cables under variable bending stiffness due to internal friction, tensile force and cable curvature", PhD Thesis, EIDGENÖSSISCHE TECHNISCHE HOCHSCHULE ZURICH, 1995

[15] D.D. Tjahjanto, A. Tyrberg, J. Mullins, "Bending mechanics of cable cores and fillers in a dynamic submarine cable", *Proceedings of the ASME 2017 36th International Conference on Ocean, Offshore and Arctic Engineering*, OMAE2017, Trondheim, Norway, June 25-30, 2017

[16] R. Nicholls-Lee, P.R. Thies, "Coupled modelling for dynamic submarine power cables – interface sensitivity analysis of global and local engineering models", *Supergen ORE Hub Annual Assembly 2021*, Poster presentation.

[17] C. Santos, C. Pesce, R. Salles, G. Franzini, R. Gonçalves, R. Morini, "An Experimental Assessment of the Hysteresis Behavior of Umbilical Cables Under Cyclic Traction", 10.1115/OMAE2017-62081, *Proceedings of the ASME 2017 36th International Conference on Ocean, Offshore and Arctic Engineering*, Trondheim, Norway, June 25-30, 2017

[15] M. Vaz, L. D'Angelo, S. Estefen, M. Brack, "Experimental determination of axial, torsional and bending stiffness of umbilical cables", *Proceedings of the ASME 1998 17th International Conference on Ocean, Offshore and Arctic Engineering*, OMAE1998